

# Maximum Cosmological Information from Type-Ia Supernova Observations

Jaiyul Yoo<sup>1,2,\*</sup>

<sup>1</sup>*Center for Theoretical Astrophysics and Cosmology, Institute for Computational Science,  
University of Zürich, Winterthurerstrasse 190, CH-8057, Zürich, Switzerland*

<sup>2</sup>*Physics Institute, University of Zürich, Winterthurerstrasse 190, CH-8057, Zürich, Switzerland*

(Dated: January 27, 2022)

Type-Ia supernova observations yield estimates of the luminosity distance, which includes not only the background luminosity distance, but also the fluctuation due to inhomogeneities in the Universe. These fluctuations are spatially correlated, hence limiting the cosmological information. In particular, the spatial correlation of the supernova host galaxies is a dominant source of the fluctuation in the luminosity distance measurements. Utilizing the recent theoretical framework that accurately quantifies the information contents accounting for the three-dimensional correlation of the observables on the past-light cone, we compute the maximum cosmological information obtainable from idealized supernova surveys, where an infinite number of observations are made over the full sky without any systematic errors up to a maximum redshift  $z_m$ . Here we consider two cosmological parameters  $\Omega_m$  and  $w_0$  and show that the cosmological information contents are a lot more reduced than previously computed in literature. We discuss how these fundamental limits set by cosmic variance can be overcome.

## I. INTRODUCTION

Measurements of type-Ia supernova provide a powerful way to probe cosmology [1, 2]. A great amount of efforts in recent decades have been devoted to increase the survey volume and reduce the intrinsic systematic errors in the luminosity distance measurements [3–7]. The error budget in supernova surveys is composed of intrinsic statistical errors due to the variation in the absolute luminosity of the individual type-Ia supernovae and systematic errors associated with the light-curve calibration. Since the former is statistical by nature, its contribution to the error budget can be reduced by increasing the number of supernova observations. The latter is, however, more difficult to quantify and control, as it depends on many uncertain factors such as the physical mechanism of the type-Ia supernova explosion, the environment of the host galaxy, and so on (see [3–7] for details). In addition, it is well-known that supernova observations yield an estimate  $D(z, \hat{n})$  of the luminosity distance that includes not only the background luminosity distance  $\bar{D}(z)$  at the observed redshift  $z$ , but also the fluctuation  $\delta D(z, \hat{n})$  at the observed position specified the angular direction  $\hat{n}$  and the redshift  $z$ , where  $D := \bar{D}(1 + \delta D)$ . The fluctuation in the luminosity distance arises, because the observed flux, the redshift, and the angular position are affected by the large-scale inhomogeneities in the Universe through the light propagation from the source to the observer. Hence, all the measurements of the luminosity distance are spatially correlated due to its fluctuations, and this correlation also contributes to the error budget.

Since the pioneering work [8], many groups showed [9–16] that the fluctuation  $\delta D$  in the luminosity distance contains the line-of-sight peculiar motion  $V$  of the host galaxy, the gravitational potential contribution  $\phi$ , and the gravitational lensing effect  $\kappa$ . The peculiar velocity is the dominant source of correlation at low redshift, while the gravitational lensing effect

takes over at higher redshift. The effects of these inhomogeneities have been investigated [10, 11, 17–20] in the past. Furthermore, since the progenitors of supernovae are associated with galaxies, supernova observations are also *biased* [12, 14], as their host galaxies are biased against the underlying matter distribution, and this fluctuation of the observed host galaxies (defined as  $\delta_g$  in Eq. [2] below) indeed constitutes the *dominant* contribution to the correlation in the supernova observations.

Therefore, in deriving the cosmological constraints from supernova surveys, it is important to take into consideration all the correlation of the luminosity distance measurements. However, previous analysis often ignored the *radial correlation* or the correlation due to the *host galaxies*. Accounting for all the effects described above, a complete theoretical formalism was derived in Ref. [21] for accurately quantifying the cosmological information contents on the light cone under the assumption that the fluctuations are at the linear order and Gaussian-distributed. In this paper, we apply this formalism to supernova surveys in the 3D light cone volume and compute the maximum cosmological information contents that are available to us in the idealized surveys, where an infinite number of supernova observations are made without any systematic errors in full sky over all redshift up to a given maximum redshift  $z_m$ .

## II. OBSERVED DATA SET

Individual observations of type-Ia supernovae yield an estimate of the luminosity distance  $D(z, \hat{n})$  at the observed redshift  $z$  and angular direction  $\hat{n}$ , but the observed data set  $\mathcal{D}(z, \hat{n})$  altogether are described as the luminosity distance  $D$  weighted by the number  $dN_g$  of the observed host galaxies in a given volume  $d\bar{V}$  determined by the redshift bin  $dz$  and the angular bin  $d^2\hat{n}$  [21]:

$$\mathcal{D}(z, \hat{n}) = D(z, \hat{n}) \frac{dN_g(z, \hat{n})}{N_g^{\text{tot}}} := \bar{D}(z) [1 + \delta \mathcal{D}(z, \hat{n})] , \quad (1)$$

\* jyoo@physik.uzh.ch

where we defined the background  $\bar{\mathcal{D}}(z)$  and the (dimensionless) fluctuation  $\delta\mathcal{D}(z, \hat{n})$  around it. In the case of one supernova observation, the total number of the observed host galaxies  $N_g^{\text{tot}} := \sum dN_g$  is unity, and the observed data set is just an estimate of the luminosity distance  $\mathcal{D}(z, \hat{n}) = D(z, \hat{n})$ . With more observations in the data set, more weight is naturally given to the estimates  $D(z, \hat{n})$  in an over-dense region, where more supernova events are observed.

It is important to note that our theoretical description  $\mathcal{D}$  in Eq. (1) is *not* the luminosity distance itself at a given position, but a description of the (discrete) observed data set in the limit  $N_g^{\text{tot}} = \infty$ . In practice, there exist a finite number of observed data points for the luminosity distance over the survey region, and the observers treat each individual point equally. For example, there will be no measurement or data point ( $\mathcal{D} = 0$ ) in the observed data set in a void, where there is no observed host galaxy ( $dN_g = 0$ ), even though the luminosity distance to such void is non-zero ( $D \neq 0$ ). This aspect of the observed data set is correctly described by Eq. (1) in the continuum limit.

The number weight  $dN_g$  is the physical number density  $n_p$  of the host galaxies times the physical volume  $dV_p$  described by the observed redshift bin  $dz$  and the angular bin  $d^2\hat{n}$ :

$$dN_g(z, \hat{n}) = n_g dV_p := \frac{d\bar{N}_g}{dz d^2\hat{n}}(z) dz d^2\hat{n} [1 + \delta_g(z, \hat{n})], \quad (2)$$

where the background part is simply the redshift distribution of the host galaxies in a homogeneous universe in terms of the Hubble parameter  $H$  and the comoving angular diameter distance  $\bar{r}$

$$\frac{d\bar{N}_g}{dz d^2\hat{n}}(z) := \frac{\bar{n}_g(z) \bar{r}^2(z)}{H(z)(1+z)^3}. \quad (3)$$

Defined as above, the fluctuation  $\delta_g(z, \hat{n})$  of the observed host galaxies is shown to be gauge-invariant [22–27], and it includes the source fluctuation (such as the galaxy bias and the magnification bias) and the volume fluctuation (such as the redshift-space distortion and the relativistic effects) [28].

Therefore, the background  $\bar{\mathcal{D}}$  and the fluctuation  $\delta\mathcal{D}$  of the observed data set are [21]

$$\bar{\mathcal{D}}(z) = \frac{\bar{D}(z)}{\bar{N}_g^{\text{tot}}} \frac{d\bar{N}_g}{dz d^2\hat{n}}(z) dz d^2\hat{n} =: \hat{\bar{\mathcal{D}}}(z) dz d^2\hat{n}, \quad (4)$$

$$1 + \delta\mathcal{D}(z, \hat{n}) = \frac{[1 + \delta D(z, \hat{n})][1 + \delta_g(z, \hat{n})]}{1 + \delta N_g^{\text{tot}}}, \quad (5)$$

where the total number  $N_g^{\text{tot}} = \bar{N}_g^{\text{tot}}(1 + \delta N_g^{\text{tot}})$  of the observed host galaxies is split into two (dimensionless) constants for later convenience

$$\bar{N}_g^{\text{tot}} := 4\pi \int_0^{z_m} dz \frac{d\bar{N}_g}{dz d^2\hat{n}}(z), \quad (6)$$

$$\delta N_g^{\text{tot}} := 4\pi \int_0^{z_m} dz \frac{1}{\bar{N}_g^{\text{tot}}} \frac{d\bar{N}_g}{dz d^2\hat{n}}(z) \int \frac{d^2\hat{n}}{4\pi} \delta_g(z, \hat{n}). \quad (7)$$

### III. SINGLE REDSHIFT BIN

We first consider supernova observations at a given redshift  $z_*$  with small redshift bin  $\Delta z$  to illustrate how individual fluctuations affect the luminosity distance estimate. The total number weight of the observed host galaxies in this case is

$$\bar{N}_g^{\text{tot}} = 4\pi \Delta z \frac{d\bar{N}_g}{dz d^2\hat{n}}, \quad \delta N_g^{\text{tot}} = \int \frac{d^2\hat{n}}{4\pi} \delta_g(\hat{n}), \quad (8)$$

directly related to the redshift distribution at the given redshift  $z_*$ , and the observed data set is then

$$\mathcal{D}(\hat{n}) = \bar{D}(z_*) \frac{d^2\hat{n}}{4\pi} [1 + \delta\mathcal{D}(\hat{n})], \quad (9)$$

where we suppressed the dependence on the survey redshift  $z_*$  and the fluctuation at the linear order in perturbations is

$$\delta\mathcal{D}(\hat{n}) \simeq \delta D(\hat{n}) + \delta_g(\hat{n}) - \delta N_g^{\text{tot}} + \mathcal{O}(2). \quad (10)$$

The number weight drops in the background part to yield  $\bar{\mathcal{D}} = \bar{D}$  up to numerical factors, as all the observed data at the same redshift are summed up. The fluctuation  $\delta\mathcal{D}$  is, however, dependent upon the fluctuation  $\delta_g$  of the host galaxies as well as the fluctuation  $\delta D$  in the luminosity distance. When averaged over the observed data set or the angle at  $z_*$ , Eq. (10) shows that  $\delta_g$  and  $\delta N_g^{\text{tot}}$  drop out

$$\delta\mathcal{D}_0 := \int \frac{d^2\hat{n}}{4\pi} \delta\mathcal{D}(\hat{n}) = \int \frac{d^2\hat{n}}{4\pi} \delta D(\hat{n}) =: \delta D_0, \quad (11)$$

though this is valid only at the linear order.

The fluctuation  $\delta D$  in the luminosity distance at the linear order is often computed in the conformal Newtonian gauge [9, 10, 12, 13]

$$\delta D(\hat{n}) \approx V_s - \frac{1+z_*}{H\bar{r}}(V_s - V_o) - \kappa, \quad (12)$$

where  $V_s$  and  $V_o$  are the line-of-sight peculiar velocity at the source and the observer positions and  $\kappa$  is the lensing convergence. Since the gravitational potential contribution to the luminosity distance is about a percent level correction to Eq. (12) (see Figure 3 in [15]), we ignored the gravitational potential contributions to  $\delta D$ . As emphasized [15, 29], the individual components in  $\delta D$  are gauge-dependent and *not* associated with any physical quantity, while the full expression for  $\delta D$  is gauge-invariant. For example,  $V_o$  should *not* be linked to the velocity we measure from the CMB dipole, because the former has different values in other gauge conditions, while the value of the latter is uniquely fixed by observations, independent of our gauge choice. Hence, one *cannot* simply remove the peculiar velocity  $V_o$  at the observer position in computing the luminosity distance, and it was shown [15] that the peculiar velocity  $V_o$  at the observer position is a dominant contribution  $V_o > V_s$  and this procedure of arbitrarily removing perturbation contributions at the observer position was the source of the infrared divergences in previous calculations [30, 31].

On a single redshift bin, the correlation of the luminosity distance fluctuation is conveniently decomposed in terms of angular power spectrum  $C_l$ ,

$$\xi_{ij} := \langle \delta \mathcal{D}(\hat{n}_i) \delta \mathcal{D}(\hat{n}_j) \rangle := \sum_l \frac{2l+1}{4\pi} C_l P_l(\gamma_{ij}), \quad (13)$$

where  $\gamma_{ij} := \hat{n}_i \cdot \hat{n}_j$  and  $P_l(x)$  is the Legendre Polynomial. Under the assumption of Gaussianity, the information contents of the observed data set for a given set of cosmological parameters  $p_\mu$  are quantified in Ref. [21] by using the Fisher matrix

$$F_{\mu\nu} = \frac{4\pi}{C_0} \left( \frac{\partial \ln \bar{D}(z_*)}{\partial p_\mu} \right) \left( \frac{\partial \ln \bar{D}(z_*)}{\partial p_\nu} \right) + \dots, \quad (14)$$

where we ignored the cosmological information contained in the correlation  $\xi_{ij}(p_\mu)$  shown as dotted in the equation and the monopole power  $C_0$  is solely determined by the peculiar velocity at the source position

$$\delta \mathcal{D}_0 = \delta D_0 = \left( 1 - \frac{1+z_*}{H\bar{r}} \right) \int \frac{d^2\hat{n}}{4\pi} V_s(\hat{n}) =: \frac{a_0}{\sqrt{4\pi}}. \quad (15)$$

The explicit expression for the monopole power  $C_0 = \langle |a_0|^2 \rangle$  is

$$C_0 = \left[ \frac{Hf}{1+z_*} \left( 1 - \frac{1+z_*}{H\bar{r}} \right) \right]^2 \frac{2}{\pi} \int dk P_\varphi(k) \mathcal{T}_m^2(k) j_0'^2(k\bar{r}), \quad (16)$$

where  $f$  is the logarithmic growth rate,  $\Delta_\varphi^2(k) := k^3 P_\varphi/2\pi^2$  is the dimensionless scalar power spectrum,  $\mathcal{T}_m(k)$  is the matter transfer function at  $z_*$ , and  $j_0(x)$  is the spherical Bessel function. With  $j_0'(x) = -j_1(x)$ , the monopole power  $C_0$  is regular in the limit  $z_* \rightarrow 0$ .

The Fisher matrix expression shows that (1) individual observations on a single redshift bin essentially yield the average over the angle and the ensemble average of the estimate is the background luminosity distance  $\bar{D}(z_*)$ , (2) the information contents depend on the sensitivity of  $\bar{D}$  to the cosmological parameters  $p_\mu$ , and (3) upon average over the sky, the estimate is limited by the cosmic variance of the monopole power  $C_0$ . In  $C_0$  (or  $a_0$ ), the host fluctuation, the lensing effect, and the velocity at the observer position completely drop out. While the correlation  $\xi_{ij}$  is a function of cosmology [32], the correlation of the luminosity distance in practice is *rarely* measured, and we ignore this contribution to the cosmological information (see, however, [32]).

#### IV. 3D LIGHT-CONE VOLUME

Supernova observations are not confined to a single redshift bin; naturally, they cover a range of redshifts, increasing the leverage to constrain cosmology. Since measurements of the luminosity distance at different redshift bins are also correlated, the increase in the cosmological constraining power is somewhat limited. A critical difference in a 3D light-cone volume is that the number weight of the host galaxies

changes in redshift, primarily due to the volume, but also due to the evolution of the host galaxies. Here we assume that the physical number density of the host galaxies evolves as  $\bar{n}_g(z) := n_0(1+z)^\alpha$ , where  $\alpha = 3$  represent a constant comoving number density such as dark matter. Compared to Eq. (9), the expectation  $\bar{D}(z)$  of the observed data set in Eq. (4) has the number weight factor, while the overall normalization constant  $n_0$  is irrelevant in our discussion.

Similarly, the number weight plays a role at the perturbation level  $\delta \mathcal{D}$ . The fluctuation  $\delta_g$  of the host galaxies is modeled here as the sum of the redshift-space distortion  $\delta_z$  [33] and the gravitational lensing effect  $\kappa$ :  $\delta_g(z, \hat{n}) \approx \delta_z - 2\kappa$ , where we ignored the velocity and the gravitational potential contributions in the full relativistic expression [27], as the density fluctuation is the dominant contribution and the lensing effect (derivatives of the gravitational potential) is comparable. For the fluctuation  $\delta D$  in the luminosity distance, we again ignore the velocity and the gravitational potential contributions to be consistent with the approximation for  $\delta_g$ :  $\delta D(z, \hat{n}) \approx -\kappa$ . Therefore, the fluctuation in the observed data set in Eq. (5) is  $\delta \mathcal{D}(z, \hat{n}) \approx \delta_z - 3\kappa - \delta N_g^{\text{tot}}$ , and its average over the sky at a given redshift is

$$\delta \mathcal{D}_0(z) \approx \int \frac{d^2\hat{n}}{4\pi} \delta_z(z, \hat{n}) - \delta N_g^{\text{tot}}(z), \quad (17)$$

where the lensing contribution again vanishes upon average. Provided that the luminosity function of the host galaxies is well-approximated by a simple power law  $\propto L^{-s}$  with the slope  $s$ , there exists an extra contribution  $(2s-1)\kappa$  in the expression  $\delta_g$  due to the magnification bias [27], but this contribution again vanishes upon average.

In a 3D light-cone volume, any observable quantities can be decomposed in terms of spherical harmonics for the angular dependence and spherical Bessel for the radial dependence [21, 34], and the correlation of the luminosity distance fluctuation is then expressed by the spherical power spectrum  $\mathcal{S}_l(k, k')$ ,

$$\begin{aligned} \xi_{ij} &= \langle \delta \mathcal{D}(z_i, \hat{n}_i) \delta \mathcal{D}(z_j, \hat{n}_j) \rangle := 4\pi \sum_{lm} \int dk \int dk' \\ &\times \frac{kk'}{2\pi^2} \mathcal{S}_l(k, k') j_l(k\bar{r}_i) j_l(k'\bar{r}_j) Y_{lm}(\hat{n}_i) Y_{lm}^*(\hat{n}_j). \end{aligned} \quad (18)$$

The spherical power spectrum is a generalization of the standard (flat-sky) power spectrum  $P(k)$ , and they are equivalent, if  $P(k)$  is *isotropic* and there is *no* evolution along the radial direction, i.e.,  $\mathcal{S}_l(k, k') = \delta^D(k - k') P(k)$ . Under the assumption that the fluctuations are Gaussian distributed, the information contents in a 3D light-cone volume can be quantified in terms of the Fisher matrix [21] as

$$F_{\mu\nu} = (4\pi)^2 \int dk \int dk' \frac{kk'}{2\pi^2} \tilde{\mathcal{S}}_0(k, k') \mathcal{G}_\mu(k) \mathcal{G}_\nu(k') + \dots, \quad (19)$$

where  $\tilde{\mathcal{S}}_l(k, k')$  is the inverse spherical power spectrum, the Fourier kernel  $\mathcal{G}_\mu(k)$  depends on cosmological parameters  $p_\mu$

$$\mathcal{G}_\mu(k) := \int_0^{z_m} dz j_0(k\bar{r}_z) \frac{\partial}{\partial p_\mu} \ln \hat{D}(z), \quad (20)$$

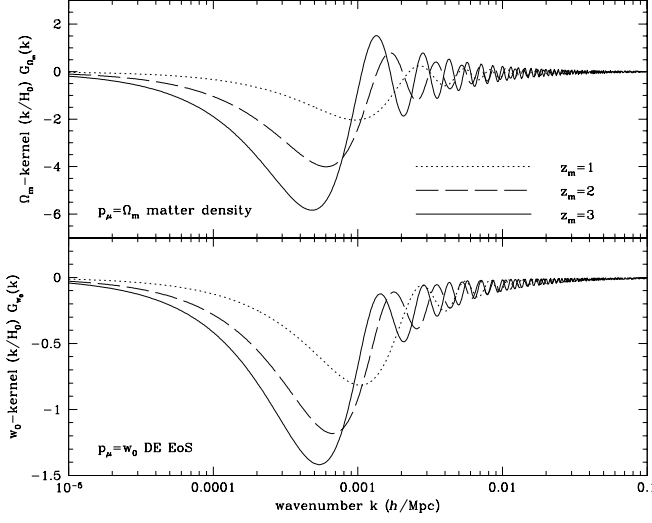


FIG. 1. Fourier kernel  $\mathcal{G}_\mu(k)$  in Eq. (20), scaled with wavevector  $k$ . The sensitivity of luminosity distance measurements in a 3D light-cone volume to cosmological parameters is represented by  $\mathcal{G}_\mu(k)$  in the Fisher matrix in Eq. (19). We consider all-sky supernova surveys with three different maximum redshifts  $z_m$  denoted as solid ( $z_m = 1$ ), dashed ( $z_m = 2$ ), and dotted ( $z_m = 3$ ).

and we again ignored the cosmological information contained in the correlation  $\xi_{ij}(p_\mu)$  shown as dotted.

Compared to the case for a single redshift bin, the Fisher matrix for a 3D light-cone volume reveals that (1) individual observations over the redshift range essentially yield  $\hat{\bar{D}}(z)$  [defined in Eq. (4)], the background luminosity distance weighted by the redshift distribution of the host galaxies, including the volume factor, (2) the information contents depend on the sensitivity of the full background quantity  $\hat{\bar{D}}(z)$  to the cosmological parameters  $p_\mu$ , *not* just the background luminosity distance  $\bar{D}(z)$ , and (3) the estimate of  $\hat{\bar{D}}(z)$  is limited by the cosmic variance described by the inverse monopole power spectrum  $\hat{\mathcal{S}}_0(k, k')$ , defined in Ref. [21] as

$$\tilde{\mathbf{S}}_l = (\mathbf{F}_l \mathbf{S}_l \mathbf{F}_l)^{-1}, \quad (21)$$

in the matrix notation, and the angular Fourier kernel is

$$\mathbf{F}_l(k, k') := \frac{2k'}{\pi} \int_0^{z_m} dz j_l(k\bar{r}_z) j_l(k'\bar{r}_z) \quad (22)$$

(see [21] for detailed derivations). For a single redshift bin, the inverse power spectrum in the Fisher matrix is *literally* the inverse of the angular power spectrum, i.e.,  $\tilde{C}_l = C_l^{-1}$ . However, for a 3D light-cone volume, the inverse power spectrum  $\hat{\mathcal{S}}_l(k, k')$  is *not* the inverse of the spherical power spectrum  $\mathcal{S}(k, k')$ , i.e.,  $\hat{\mathcal{S}}_l(k, k') \neq \mathcal{S}_l^{-1}(k, k')$ , as apparent in the matrix inversion relation in Eq. (21). The reason is that the evolution along the light cone mixes different Fourier modes and the survey volume is finite, rather than an infinite hyper-surface.

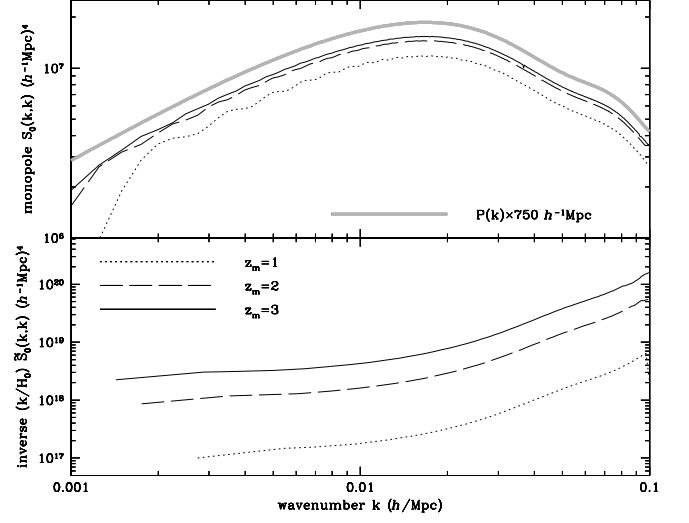


FIG. 2. Monopole  $\mathcal{S}_0(k, k)$  and inverse monopole  $\hat{\mathcal{S}}_0(k, k)$  power spectra for the surveys with three different maximum redshifts shown in the legend. Only the diagonal parts of the monopole spectra are plotted. *Upper*: The monopole spherical power spectra  $\mathcal{S}_0(k, k)$  is plotted with three  $z_m$ . As a reference, the gray curve shows the matter power spectrum  $P_m(k)$  at redshift zero, scaled with  $750 h^{-1} \text{Mpc}$ . *Lower*: The inverse monopole power spectra  $\hat{\mathcal{S}}_0(k, k)$  with three  $z_m$  is shown.  $\hat{\mathcal{S}}_0(k, k)$  are scaled with wavenumber to highlight the contribution to the Fisher matrix in Eq. (27).

Using Eq. (17), the monopole power spectrum can be computed as

$$\mathcal{S}_0(k, k') = 4\pi \int d\ln \tilde{k} \Delta_\varphi^2(\tilde{k}) \left[ \mathcal{M}_0^{\delta_z}(k, \tilde{k}) - \mathcal{M}_0^{\delta N_g^{\text{tot}}}(k, \tilde{k}) \right] \times \left[ \mathcal{M}_0^{\delta_z}(k', \tilde{k}) - \mathcal{M}_0^{\delta N_g^{\text{tot}}}(k', \tilde{k}) \right], \quad (23)$$

where the Fourier kernels for the angle-averaged redshift-space distortion and the fluctuation in the number weight are

$$\mathcal{M}_0^{\delta_z}(k, \tilde{k}) := k \sqrt{\frac{2}{\pi}} \int_0^{\bar{r}_m} d\bar{r} \bar{r}^2 j_0(k\bar{r}) \mathcal{T}_z(\tilde{k}; \bar{r}), \quad (24)$$

$$\mathcal{M}_0^{\delta N_g^{\text{tot}}}(k, \tilde{k}) := k \sqrt{\frac{2}{\pi}} \int_0^{\bar{r}_m} d\bar{r} \bar{r}^2 j_0(k\bar{r}) \times 4\pi \int_0^{z_m} dz \frac{1}{\bar{N}_g^{\text{tot}}} \frac{d\bar{N}_g}{dz d^2 \hat{n}} \mathcal{T}_z(\tilde{k}; z), \quad (25)$$

$$\mathcal{T}_z(k; \bar{r}) := \left[ \left( b + \frac{1}{3}f \right) j_0(k\bar{r}) - \frac{2f}{3} j_2(k\bar{r}) \right] \mathcal{T}_m(k; \bar{r}), \quad (26)$$

and  $\bar{r}_m := \bar{r}(z_m)$ . The dependence of the redshift-space distortion kernel  $\mathcal{T}_z(k)$  on  $l = 0$  and  $l = 2$  arises due to the dependence on  $\mu_k^2$  of  $\delta_z(k) = (b + f\mu_k^2)\delta_m(k)$ , where  $b$  is the galaxy bias factor,  $\mu_k := \hat{n} \cdot \hat{k}$ , and  $f$  is the logarithmic growth rate. The kernels  $\mathcal{M}_0(k, \tilde{k})$  represent the contributions to the angle average in Eq. (17), and they are not symmetric in arguments.

## V. NUMERICAL COMPUTATION

To be specific, we adopt the best-fit  $\Lambda$ CDM model cosmological parameters presented in Table 7 (Planck alone) of the *Planck* 2018 result [35]. For simplicity, we first assume that the host galaxies are described by the matter distribution ( $b = 1$  and  $\alpha = 3$ ), and we ignore the redshift-space distortion ( $f \equiv 0$ ). Figure 1 shows the Fourier kernels  $\mathcal{G}_\mu(k)$  for two cosmological parameters with three different maximum redshifts  $z_m$  of idealized supernova surveys. The kernel  $\mathcal{G}_\mu(k)$  multiplied by a wavenumber contributes to the Fisher matrix  $F_{\mu\nu}$  in Eq. (19), and the product is bounded at all  $k$ , exhibiting the peak contribution around the characteristic scale of the survey depth  $k \approx 2/\bar{r}_m$ . Compared to  $\partial \ln \bar{D}/\partial p_\mu$  in the single redshift bin, the log-derivative in  $\mathcal{G}_\mu(k)$  includes the volume factor, which enhances the sensitivity by about factor two at a given redshift. The dependence of the evolution slope  $\alpha$  is rather weak, only through the total number  $\bar{N}_g^{\text{tot}}$  for  $\mathcal{G}_\mu(k)$ .

The upper panel of Figure 2 shows the spherical monopole power spectra  $\mathcal{S}_0(k, k)$  with three  $z_m$ . The Fourier kernels  $\mathcal{M}_0(k, \tilde{k})$  for  $\mathcal{S}_0(k, \tilde{k})$  behaves like a Dirac delta function due to two spherical Bessel functions in the kernels. Consequently,  $\mathcal{S}_0(k, \tilde{k})$  is *nearly* diagonal. In the limit  $k \rightarrow \infty$ , where the survey depth is comparatively large  $\bar{r}_m \gg 1/k$ , the integrals in Eqs. (24) and (25) can be performed analytically by ignoring the time-evolution of the transfer function  $\mathcal{T}_m(k; \bar{r})$  to yield  $\tilde{\mathcal{S}}_0(k, k') \approx \delta^D(k - k') b^2 P_m(k)$ , where  $P_m$  is the matter power spectrum averaged over the survey depth. Since  $\delta^D(k - k')$  in  $\mathcal{S}_0(k, k)$  is proportional to  $\bar{r}_m$ , the monopole power  $\mathcal{S}_0(k, k)$  with  $z_m = 3$  is largest among three, while the averaged matter power spectrum with  $z_m = 3$  is lowest among three. For a reference, the matter power spectrum today is plotted as a gray curve, illustrating the similarity to  $\mathcal{S}_0(k, k)$  at  $k\bar{r}_m \gg 1$ . At low  $k$ , the power in  $\mathcal{S}_0(k, k)$  is reduced due to the survey volume.

The lower panel in Figure 2 shows the inverse monopole power spectra  $\tilde{\mathcal{S}}_0(k, k)$ , scaled with a wavevector. Since  $\mathcal{S}_0(k, k')$  is nearly diagonal,  $\tilde{\mathcal{S}}_0(k, k')$  in Eq. (21) is nearly diagonal as well. However, the inverse spectrum  $\tilde{\mathcal{S}}_0(k, k')$  is defined only for the wave numbers that are approximately measurable in a given survey, i.e.,  $k\bar{r}_m \gtrsim 1$ . For any long wavelength modes ( $k\bar{r}_m \ll 1$ ), the spherical power spectrum  $\mathcal{S}_0(k, k)$  has approximately the same value close to zero, hence the matrix  $\mathbf{S}_0$  is *not* invertible, as the spherical Bessel functions vary little for those wave numbers over the survey volume. So  $\tilde{\mathcal{S}}_0(k, k)$  is plotted only for  $k \geq 2\pi/\bar{r}_m$ . The inverse spherical power is very flat over the survey scales. Since  $\tilde{\mathcal{S}}_0(k, k')$  is nearly diagonal, the Fisher matrix in Eq. (19) can be re-arranged as

$$F_{\mu\nu} \approx 8 \int d \ln k \left[ \int dk' k \tilde{\mathcal{S}}_0(k, k') \right] k \mathcal{G}_\mu(k) k \mathcal{G}_\nu(k), \quad (27)$$

illustrating that the cosmological information is proportional to the Fourier kernel  $k \mathcal{G}_\mu(k)$  in Figure 1 and the inverse power spectrum  $k \tilde{\mathcal{S}}_0(k, k)$  in Figure 2. For numerical computation of  $F_{\mu\nu}$  in Eq. (19), we compute the full matrices  $\mathbf{S}_0$  and  $\tilde{\mathbf{S}}_0$ .

Figure 3 illustrates the minimum fractional errors on two

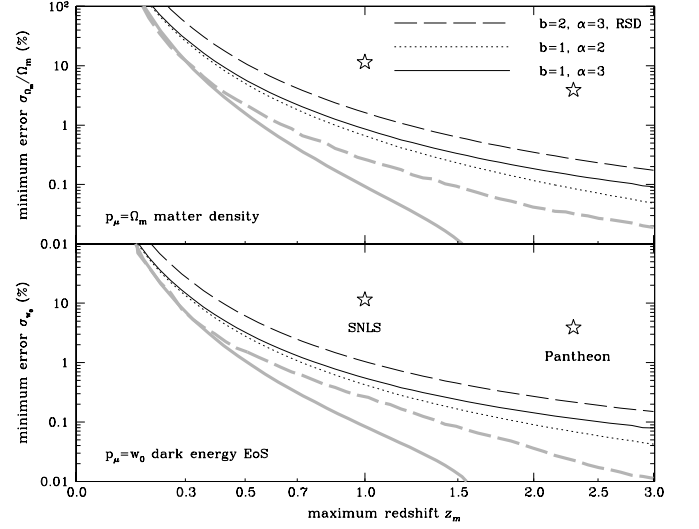


FIG. 3. Minimum fractional errors on two cosmological parameters from idealized supernova surveys alone that measure infinite number of supernova events without any systematic errors up to the maximum redshift  $z_m$ . The correlation of the fluctuations in the luminosity distance and the host galaxies limits our ability to measure the cosmological parameters precisely in the surveys. Various curves illustrate the dependence of the model parameters associated with the host galaxies. Gray curves show the change, if we ignore the radial correlation (solid) or the host galaxy fluctuation (dashed). They represent the past (imprecise) forecasts in literature.

cosmological parameters from idealized supernova surveys. The minimum errors decrease with  $z_m$ , as more volume is included in the surveys. Compared to our fiducial model (solid), host galaxies with higher bias ( $b = 2$ ; dashed) are more correlated, reducing our leverage to constrain the cosmological parameters, and the increase in the minimum errors are about the ratio of the (constant) bias factors. As type-Ia supernovae occur in a highly biased region (described by the bias factor in our model) such as massive galaxies or clusters of galaxies rather than field galaxies, the observed data set from supernova surveys probes only the biased region of the Universe, and its constraints deviate more from the cosmic mean. The redshift-space distortion (RSD) also increases the correlation of the host galaxies, though its impact is minor, as the logarithmic growth rate  $f$  is small and two terms with  $f$  in Eq. (26) are partially cancelled. The host galaxies whose number density increases in time ( $\alpha = 2$ ; dotted) effectively put more weight on the lower redshift populations and increase  $\delta N_g^{\text{tot}}(z)$ , reducing the fluctuation in the observed data set in Eq. (17). But its impact is small and visible only when the redshift depth is large.

Gray curves illustrate the change in the forecast, if the radial correlation (solid) or the host galaxy correlation (dashed) is ignored. These cases represent the current status in literature. In the former, the survey volume is split into multiple redshift bins with width  $\Delta z = 0.05$ , and the Fisher matrix in Eq. (14) for each redshift bin are added, as if each redshift bin is independent. This procedure of ignoring the radial cor-

relation *significantly underestimates* the cosmic variance and hence the minimum errors. In fact, the results depend on the bin width  $\Delta z$  or the number of “independent” redshift bins. When the host galaxy fluctuation is ignored ( $\delta_g \equiv 0$ , dashed gray), the observed data set Eq. (5) is simplified as  $\delta\mathcal{D} = \delta D$ , and the Fourier kernel for the monopole power spectrum is

$$\mathcal{M}_0^V(k, \tilde{k}) = \sqrt{\frac{2}{\pi}} k \int d\bar{r} \bar{r}^2 j_0(k\bar{r}) \frac{j'_0(\tilde{k}\bar{r})}{\tilde{k}\bar{r}} (\mathcal{H}\bar{r}-1) f \mathcal{T}_m(\tilde{k}; \bar{r}), \quad (28)$$

where we used Eq. (12) and there is no contribution of  $\kappa$  or  $V_0$  to the monopole power. While the radial correlation is properly considered, the dominant source (or  $\delta_g$ ) of the correlation is missing, and this assumption still *underestimates* the minimum errors.

Two symbols in Figure 3 show the current errors from the Pantheon sample [7] with  $z_m \simeq 2.3$  and the Supernova Legacy Survey (SNLS; [5]) with  $z_m \simeq 1.0$ . The errors from both surveys in Figure 3 are those reported in the collaboration papers [5, 7], in which they combined the supernova observations with the *Planck* CMB analysis. The intrinsic scatter associated with individual supernovae is a dominant contribution to their error budget, which we set zero in idealized surveys considered here. Moreover, while the correlation of the peculiar velocities is approximately accounted for in the analysis [5, 7], the correlation of the host galaxies is ignored. While the fundamental limit set by the cosmic variance is yet to be reached in these surveys at high redshift, its impact is more significant at lower redshift.

## VI. DISCUSSION

Accounting for the correct correlation of the luminosity distance measurements, we derived the *precise* minimum errors on two cosmological parameters from idealized supernova surveys, where an infinite number of supernova observations are made without any systematic errors. The minimum floors exist because the light propagation from individual supernovae is affected by large-scale inhomogeneities and the host galaxies are also correlated. However, past work in literature ignored the radial correlation along the past light cone

or the contribution of the supernova host galaxies. With all the correlations properly accounted for, we find that the luminosity distance measurements are more correlated and the cosmological constraining power is more reduced than previously estimated.

Today, the systematic errors associated with the light-curve calibration are the limiting factors in the current supernova surveys, and they cannot be beaten down by increasing the number of observations in future surveys. Our results from idealized supernova surveys without such systematic errors, however, provide fundamental limitations set by the cosmic variance, regardless of the survey specifications in the future. In practice, one would have to consider both contributions in designing a supernova survey. Apparent from Figure 3, the cosmic variance is more important at low redshift, where only a small fraction of the Universe can be probed.

Though we assumed perfect knowledge of  $\Delta_\phi^2$ ,  $\mathcal{T}_m$ ,  $b$ ,  $\alpha$ , and  $f$  for the computation, their uncertainties in practice would also degrade the cosmological constraining power. In particular, the bias factor for the supernova host galaxies is expected to be different from that of typical galaxies, and its theoretical modeling is highly uncertain. While the second-order fluctuations from inhomogeneities will break our assumption of Gaussianity, its impact is largely limited to shifting the best-fit cosmological parameters at a percent level [20], and hence we believe that the impact on the cosmic variance is similar in magnitude. While the real surveys are yet to reach the limits considered here, there are several ways to extract more information and overcome the limits in Figure 3. The spatial correlation  $\xi_{ij}$  of individual observations contains cosmological information that can be harnessed, but was ignored in Figure 3. Cross correlation with other galaxy populations in the same volume provides a way to beat the cosmic variance and reduce the errors [36].

## ACKNOWLEDGMENTS

We thank Ermis Mitsou for useful discussions. We acknowledge support by the Swiss National Science Foundation. J.Y. is further supported by a Consolidator Grant of the European Research Council (ERC-2015-CoG grant 680886).

- 
- [1] A. G. Riess et al., *Astron. J.* **116**, 1009 (1998), arXiv:astro-ph/9805201.
  - [2] S. Perlmutter et al., *Astrophys. J.* **517**, 565 (1999), arXiv:astro-ph/9812133.
  - [3] R. Kessler, A. C. Becker, D. Cinabro, J. Vanderplas, J. A. Frieman, J. Marriner, et al., *Astrophys. J. Suppl. Ser.* **185**, 32 (2009), 0908.4274.
  - [4] M. Sullivan, J. Guy, A. Conley, N. Regnault, P. Astier, et al., *Astrophys. J.* **737**, 102 (2011), 1104.1444.
  - [5] M. Betoule, R. Kessler, J. Guy, J. Mosher, D. Hardin, et al., *Astron. Astrophys.* **568**, A22 (2014), 1401.4064.
  - [6] G. Narayan, A. Rest, B. E. Tucker, R. J. Foley, W. M. Wood-Vasey, et al., *Astrophys. J. Suppl. Ser.* **224**, 3 (2016), 1603.03823.
  - [7] D. M. Scolnic, D. O. Jones, A. Rest, Y. C. Pan, R. Chornock, et al., *Astrophys. J.* **859**, 101 (2018), 1710.00845.
  - [8] M. Sasaki, *Mon. Not. R. Astron. Soc.* **228**, 653 (1987).
  - [9] C. Bonvin, R. Durrer, and M. A. Gasparini, *Phys. Rev. D* **73**, 023523 (2006), arXiv:0511183.
  - [10] L. Hui and P. B. Greene, *Phys. Rev. D* **73**, 123526 (2006), astro-ph/0512159.
  - [11] C. Clarkson, G. F. R. Ellis, A. Faltenbacher, R. Maartens, O. Umeh, and J.-P. Uzan, *Mon. Not. R. Astron. Soc.* **426**, 1121 (2012), 1109.2484.
  - [12] N. Kaiser and M. J. Hudson, *Mon. Not. R. Astron. Soc.* **450**, 883 (2015), 1411.6339.

- [13] J. Yoo and F. Scaccabarozzi, *J. Cosmol. Astropart. Phys.* **9**, 046 (2016), 1606.08453.
- [14] P. Fleury, C. Clarkson, and R. Maartens, *J. Cosmol. Astropart. Phys.* **2017**, 062 (2017), 1612.03726.
- [15] S. G. Biern and J. Yoo, *J. Cosmol. Astropart. Phys.* **4**, 045 (2017), 1606.01910.
- [16] F. Scaccabarozzi and J. Yoo, *J. Cosmol. Astropart. Phys.* **6**, 007 (2017), 1703.08552.
- [17] C. Bonvin, R. Durrer, and M. Kunz, *Phys. Rev. Lett.* **96**, 191302 (2006), astro-ph/0603240.
- [18] I. Ben-Dayan, M. Gasperini, G. Marozzi, F. Nugier, and G. Veneziano, *J. Cosmol. Astropart. Phys.* **4**, 036 (2012), 1202.1247.
- [19] I. Ben-Dayan, M. Gasperini, G. Marozzi, F. Nugier, and G. Veneziano, *Phys. Rev. Lett.* **110**, 021301 (2013), 1207.1286.
- [20] I. Ben-Dayan, R. Durrer, G. Marozzi, and D. J. Schwarz, *Phys. Rev. Lett.* **112**, 221301 (2014), 1401.7973.
- [21] J. Yoo, E. Mitsou, N. Grimm, R. Durrer, and A. Refregier, *J. Cosmol. Astropart. Phys.* **2019**, 015 (2019), 1905.08262.
- [22] J. Yoo, A. L. Fitzpatrick, and M. Zaldarriaga, *Phys. Rev. D* **80**, 083514 (2009), arXiv:0907.0707.
- [23] J. Yoo, *Phys. Rev. D* **82**, 083508 (2010), arXiv:1009.3021.
- [24] C. Bonvin and R. Durrer, *Phys. Rev. D* **84**, 063505 (2011), arXiv:1105.5280.
- [25] A. Challinor and A. Lewis, *Phys. Rev. D* **84**, 043516 (2011), arXiv:1105.5292.
- [26] D. Jeong, F. Schmidt, and C. M. Hirata, *Phys. Rev. D* **85**, 023504 (2012), arXiv:1107.5427.
- [27] J. Yoo, *Class. Quant. Grav.* **31**, 234001 (2014), arXiv:1409.3223.
- [28] J. Yoo, *Phys. Rev. D* **79**, 023517 (2009), arXiv:0808.3138.
- [29] F. Scaccabarozzi, J. Yoo, and S. G. Biern, *J. Cosmol. Astropart. Phys.* **10**, 024 (2018), 1807.09796.
- [30] E. Barausse, S. Matarrese, and A. Riotto, *Phys. Rev. D* **71**, 063537 (2005), astro-ph/0501152.
- [31] E. W. Kolb, S. Matarrese, A. Notari, and A. Riotto, *Phys. Rev. D* **71**, 023524 (2005), hep-ph/0409038.
- [32] S. G. Biern and J. Yoo, *J. Cosmol. Astropart. Phys.* 026 (2017), 1704.07380.
- [33] N. Kaiser, *Mon. Not. R. Astron. Soc.* **227**, 1 (1987).
- [34] J. Yoo and V. Desjacques, *Phys. Rev. D* **88**, 023502 (2013), 1301.4501.
- [35] Planck Collaboration et al., arXiv e-prints (2018), 1807.06205.
- [36] U. Seljak, *Phys. Rev. Lett.* **102**, 021302 (2009), 0807.1770.